ARTICLES

Kinetics of a mixed Ising ferrimagnetic system

G. M. Buendía

Departamento de Física, Universidad Simón Bolívar, Apartado 89000, Caracas 1080, Venezuela

E. Machado

Departamento de Física, Universidad Simón Bolívar, Apartado 89000, Caracas 1080, Venezuela
and Departamento de Física, Universidad Central de Las Villas, Santa Clara 4300, Cuba

(Received 2 December 1997; revised manuscript received 12 March 1998)

We present a study, within a mean-field approach, of the kinetics of a classical mixed Ising ferrimagnetic model on a square lattice, in which the two interpenetrating square sublattices have spins $\sigma = \pm 1/2$ and $S = \pm 1, 0$. The kinetics is described by a Glauber-type stochastic dynamics in the presence of a time-dependent oscillating external field and a crystal field interaction. We can identify two types of solutions: a symmetric one, where the total magnetization M oscillates around zero, and an antisymmetric one where M oscillates around a finite value different from zero. There are regions of the phase space where both solutions coexist. The dynamical transition from one regime to the other can be of first or second order depending on the region in the phase diagram. Depending on the value of the crystal field we found up to two dynamical tricritical points where the transition changes from continuous to discontinuous. Also, we perform a similar study on the Blume-Capel ($S = \pm 1, 0$) model and find strong differences between its behavior and the one of the mixed model. [S1063-651X(98)05107-1]

PACS number(s): 05.50.+q, 75.10.Hk

I. INTRODUCTION

The time evolution of metastable states of a mixed Ising ferrimagnetic model is studied by establishing a Glauber-type dynamic [1] that drives the system between two equivalent ordered phases. This approach provides a simple way to introduce a nonequilibrium kinetics into models such as the Ising and the Ising mixed systems, that do not have a deterministic dynamics. Numerous studies indicate that stochastic dynamics, despite its simplicity, can describe in a qualitatively correct way nonequilibrium phenomena and dynamical phase transitions found in real systems [2]. A kinetic Ising model has been applied successfully to model magnetization switching in nanoscale ferromagnets [3].

The model to be studied is a mixed Ising ferrimagnetic system on a square lattice in which the two interpenetrating sublattices have spins one-half ($\pm 1/2$) and spins one ($\pm 1, 0$). This system is relevant for understanding bimetallic molecular ferrimagnets that are currently being synthesized by several experimental groups in search of stable, crystalline materials, with spontaneous magnetic moments at room temperature [4]. The magnetic properties of the mixed Ising models have been studied by high-temperature series expansions [5], renormalization group [6], mean field [7], Monte Carlo simulations, and numerical transfer matrix calculations [8], but always at equilibrium conditions.

In this work we are going to study, within a mean-field approach, the kinetics of the model in the presence of a time-dependent oscillating external field. We found that there are three regimes: a paramagnetic one where the total magnetization follows the field, a ferromagnetic one where the total

magnetization does not follow the field and oscillates around a value different from zero, and a region where both solutions coexist. The transition between regimes can be continuous or discontinuous, depending on the temperature and the external field. Depending on the parameters of the Hamiltonian this system can have up to two dynamical tricritical points.

II. THE MODEL

We consider a kinetic mixed Ising ferrimagnetic system in a square lattice described by the Hamiltonian

$$\mathcal{H} = -J \sum_{\langle NN \rangle} S_i \sigma_j - D \sum_i S_i^2 - H \left(\sum_i S_i + \sum_j \sigma_j \right), \quad (1)$$

where the S_i take the values ± 1 or 0 and are located in alternating sites with spins $\sigma_j = \pm 1/2$. Each spin S has only σ spins as nearest neighbors and vice versa. The sum $\sum_{\langle NN \rangle}$ is carried out over all nearest-neighbor pairs. The sums $\sum_i$ and $\sum_j$ run over all the sites of the S and σ sublattices, respectively. J is the exchange parameter, D is the crystal field interaction, and H is a time-dependent external magnetic field given by

$$H(t) = H_0 \cos(\omega t), \quad (2)$$

all in energy units. We choose J to be negative, so the coupling between the NN spins is antiferromagnetic.

The system evolves according to a Glauber-type stochastic dynamics at a rate of $1/\tau$ transitions per unit time. Leaving the S spins fixed, we define $P'(\sigma_1, \ldots, \sigma_N; t)$ as the

probability that the system has the σ-spin configuration, $\sigma_1, \ldots, \sigma_N$, at time t, also, by leaving the σ spins fixed, we define $P''(S_1, \ldots, S_N; t)$ as the probability that the system has the S-spin configuration, $S_1, \ldots, S_N$, at time t. Then, we calculate $w_j(\sigma_j)$ and $W_i(S_i \to S_i')$, the probabilities per unit time that the jth σ spin changes from σ_j to $-\sigma_j$ and the ith S spin changes from S_i to S_i', respectively.

A. Calculation of $w_j(\sigma_j)$

We write the time derivative of $P'(\sigma_1, \ldots, \sigma_N; t)$ as

$$\frac{d}{dt} P'(\sigma_1, \ldots, \sigma_N; t)$$

$$= -\left(\sum_j w_j(\sigma_j) \right) P'(\sigma_1, \ldots, \sigma_j, \ldots, \sigma_N; t)$$

$$+ \sum_j w_j(-\sigma_j) P'(\sigma_1, \ldots, -\sigma_j, \ldots, \sigma_N; t). \quad (3)$$

If the system is in contact with a heat bath at temperature T, each spin σ can flip with probability per unit time given by the Boltzmann factor [9]

$$w_j(\sigma_j) = \frac{1}{\tau} \frac{\exp(-\beta \Delta E_j')}{1 + \exp(-\beta \Delta E_j')}, \quad \beta = 1/k_B T \quad (4)$$

where

$$\Delta E_j' = 2\sigma_j \left(J \sum_{\langle i \rangle} S_i + H \right) \quad (5)$$

gives the change in the energy of the system when the σ_j-spin flips.

From the master equation associated to the stochastic process it is simple to prove that the average $\langle \sigma_j(t) \rangle$ satisfies the equation [10]

$$\tau \frac{d}{dt} \langle \sigma_j \rangle = -\langle \sigma_j \rangle + \left\langle \frac{1}{2} \tanh \left[\frac{1}{2} \beta \left(J \sum_{\langle i \rangle} S_i + H \right) \right] \right\rangle, \quad (6)$$

that, within a mean-field approach [11] and for an external field defined by Eq. (2), takes the form

$$\tau \frac{d}{dt} \langle \sigma \rangle = -\langle \sigma \rangle + \frac{1}{2} \tanh \frac{1}{2} \beta [JZ\langle S \rangle + H_0 \cos(\omega t)], \quad (7)$$

where $\langle \sigma \rangle$ and $\langle S \rangle$ are the σ-spin and S-spin sublattice magnetizations, respectively, and $Z = 4$ is the coordination number for this model.

B. Calculation of $W_i(S_i \to S_i')$

In a similar way, the time derivative of the $P''(S_1, \ldots, S_N; t)$ can be written as

$$\frac{d}{dt} P''(S_1, \ldots, S_N; t)$$

$$= -\sum_i \left(\sum_{S_i' \neq S_i} W_i(S_i \to S_i') \right) P''(S_1, \ldots, S_N; t)$$

$$+ \sum_i \left(\sum_{S_i' \neq S_i} W_i(S_i' \to S_i) P''(S_1, \ldots, S_i', \ldots, S_N; t) \right). \quad (8)$$

Each spin can change from the value S_i to the value S_i' with probability per unit time

$$W_i(S_i \to S_i') = \frac{1}{\tau} \frac{\exp[-\beta \Delta E''(S_i \to S_i')]}{\sum_{S_i'} \exp[-\beta \Delta E''(S_i \to S_i')]}, \quad (9)$$

where $\Sigma_{S_i'}$ is the sum over the three possible values of S_i', $\pm 1, 0$, and

$$\Delta E''(S_i \to S_i') = -(S_i' - S_i) \left(J \sum_{\langle j \rangle} \sigma_j + H \right) - (S_i'^2 - S_i^2) D \quad (10)$$

gives the change in the energy of the system when the S_i-spin changes. The probabilities satisfy the detailed balance condition

$$\frac{W_i(S_i \to S_i')}{W_i(S_i' \to S_i)} = \frac{P''_{eq}(S_1, \ldots, S_i', \ldots, S_N)}{P''_{eq}(S_1, \ldots, S_i, \ldots, S_N)} \quad (11)$$

and, substituting the possible values of S_i, we get

$$W_i(1 \to 0) = W_i(-1 \to 0) = \frac{\exp(-\beta D)}{2\cosh a + \exp(-\beta D)},$$

$$W_i(1 \to -1) = W_i(0 \to -1) = \frac{\exp(-a)}{2\cosh a + \exp(-\beta D)},$$

$$(12)$$

$$W_i(0 \to 1) = W_i(-1 \to 1) = \frac{\exp(a)}{2\cosh a + \exp(-\beta D)},$$

where $a = \beta(J\Sigma_{\langle j \rangle} \sigma_j + H)$. Notice that, since $W_i(S_i \to S_i')$ does not depend on S_i, we can write $W_i(S_i \to S_i') = W_i(S_i')$, and the master equation becomes

$$\frac{d}{dt} P''(S_1, \ldots, S_N; t)$$

$$= -\sum_i \left(\sum_{S_i' \neq S_i} W_i(S_i') \right) P''(S_1, \ldots, S_N; t)$$

$$+ \sum_i W_i(S_i) \left(\sum_{S_i' \neq S_i} P''(S_1, \ldots, S_i', \ldots, S_N; t) \right). \quad (13)$$
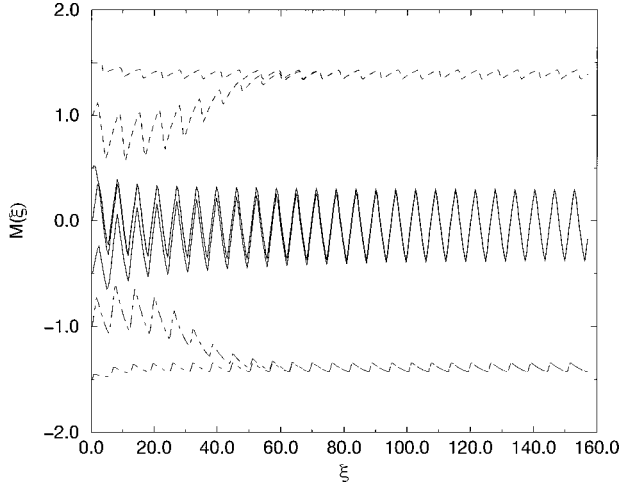
FIG. 1. Solutions for different initial conditions with $T=0.05$, $h=0.5$, $\Omega/2\pi=1.0$, and $D=20$. As we see, after the transient regime, some different initial conditions give the same solutions.

Since the sum of probabilities is normalized to one, by multiplying both sides of Eq. (13) by S_k and taking the average, we obtain

$$\tau\frac{d}{dt}\langle S_k\rangle = -\langle S_k\rangle + \frac{2\sinh\beta\left(J\sum_{\langle j\rangle}\sigma_j + H\right)}{2\cosh\beta\left(J\sum_{\langle j\rangle}\sigma_j + H\right) + \exp(-\beta D)}$$

(14)

or, in terms of a mean-field approach

$$\tau\frac{d}{dt}\langle S\rangle = -\langle S\rangle$$
$$+ \frac{2\sinh\beta[JZ\langle\sigma\rangle + H_0\cos(\omega t)]}{2\cosh\beta[JZ\langle\sigma\rangle + H_0\cos(\omega t)] + \exp(-\beta D)}.$$

(15)

III. RESULTS

The system evolves according to the set of coupled differential equations given by Eqs. (7) and (15), that can be written in the form

$$\Omega\frac{d}{d\xi}m_1 = -m_1 + \frac{\sinh(1/T)(m_2 + h\cos\xi)}{\cosh(1/T)(m_2 + h\cos\xi) + \frac{1}{2}\exp(-\beta D)},$$

(16)

$$\Omega\frac{d}{d\xi}m_2 = -m_2 + \frac{1}{2}\tanh\frac{1}{2T}(m_1 + h\cos\xi),$$

where $m_1 = \langle S\rangle$ and $m_2 = \langle\sigma\rangle$, $\Omega = \tau\omega$, $\xi = \omega t$, $T = (\beta JZ)^{-1}$, and $h = H_0/JZ$. We fix $J = -1$. We are going to study the stationary solutions of this system and its dependence with the parameters.

In general, the solutions of the system depend on the initial conditions $m_1(\xi=0)$ and $m_2(\xi=0)$. For a given set of parameters and initial conditions the system passes through a
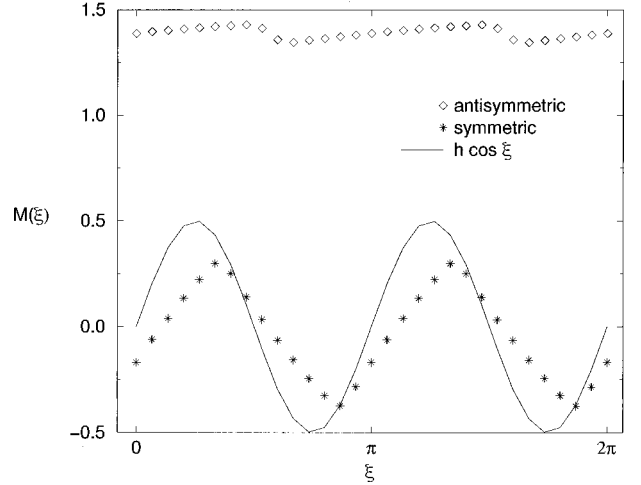

FIG. 2. Types of solutions: antisymmetric where M oscillates around a finite value different from zero, and symmetric where M oscillates around zero. For $T=0.05$, $h=0.5$, $\Omega/2\pi=1.0$, and $D=20$.

transient regime until the solution becomes stationary. In Fig. 1, we show the solutions of the total magnetization, $M = m_1 + m_2$, for different initial conditions. We found that the following combinations of initial conditions:

$$m_1(\xi=0) = 1, \quad m_2(\xi=0) = 0.5,$$

(17)

$$m_1(\xi=0) = 0, \quad m_2(\xi=0) = 0$$

(18)

give all the possible different stationary solutions. As expected, the sublattice magnetizations, m_1, m_2, and the total magnetization M are periodic functions of ξ with period 2π.

By choosing as the dynamical parameter the average total magnetization in a period

$$Q = \frac{1}{2\pi}\int_0^{2\pi} M(\xi)d\xi$$

(19)

we can identify two types of solutions: a symmetric one where $M(\xi)$ follow the field, oscillating around zero giving $Q=0$, and an antisymmetric one where $M(\xi)$ does not follow the field and oscillates around a finite value different from zero, such that $Q\neq 0$. Examples of both types of solutions are shown in Fig. 2. The first type of solution is called paramagnetic (P) and the second type ferromagnetic (F). The dynamical phase transition is located in the boundary between both solutions, and depending on the region of the phase diagram, can be of first or second order. For the first order phase transition the order parameter Q is discontinuous, and jumps abruptly from zero to a nonzero value. For the second order phase transition, the order parameter decreases continuously to zero, but its first derivative is discontinuous. If we fix the values of D and Ω for each value of h, we get that the dynamical phase transition occurs at temperature T_c. In the thermodynamical plane, (T,h), we can define a critical line $T_c = T_c(h)$, the point on the critical line at which the transition changes from first order to second order is denominated dynamical tricritical point.

As it is shown in Fig. 3, for D large and positive, we recover the phase diagram of the standard Ising model [11].
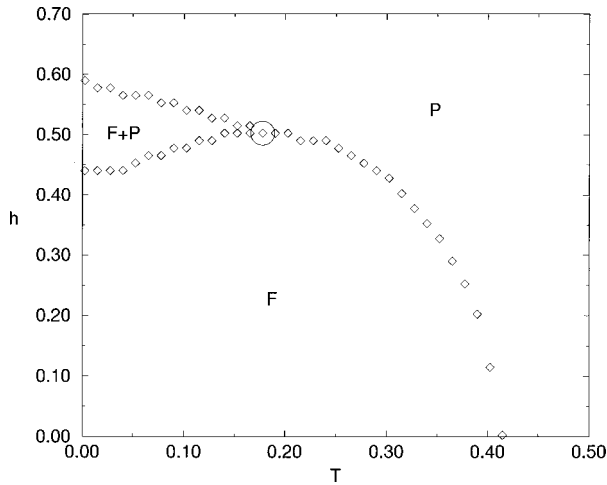
FIG. 3. Phase diagram in the (T,h) plane for $\Omega/2\pi = 1.0$ and $D = 20.0$. The paramagnetic (P) and the ferromagnetic (F) solutions overlap in the region indicated by P+F. The $\bigcirc$ symbol indicates the dynamical tricritical point.

FIG. 5. Behavior of $m_1(\xi)$ and $m_2(\xi)$ for $T = 0.05$, $h = 0.2$, $\Omega/2\pi = 1.0$, and $D = -1.5$.

At high temperatures the solutions are paramagnetic and at low temperatures they are ferromagnetic. The boundary between both regions, F$\rightarrow$P, is given by the critical line, and indicates a continuous phase transition. At low temperatures, there is a range of values of h for which the ferromagnetic and paramagnetic solutions coexist and two separated critical lines appear, one that indicates the discontinuous transition between the F and the P+F regions, and the other that indicates the discontinuous transition between the P+F and the P regions. The point where both lines merge signals the change from a first order to a second order phase transition and is a dynamical tricritical point.

When D becomes negative, we found that in the range $-2.037\,60 \leqslant D < -0.118\,25$ (for $\Omega/2\pi = 1$) and low temperatures, a new first order critical line appears that separates a new region where both solutions coexist F+P from the F region. A phase diagram corresponding to a value of D in this interval is shown in Fig. 4. This new critical line is due to the fact that, in this region, the sublattice magnetization
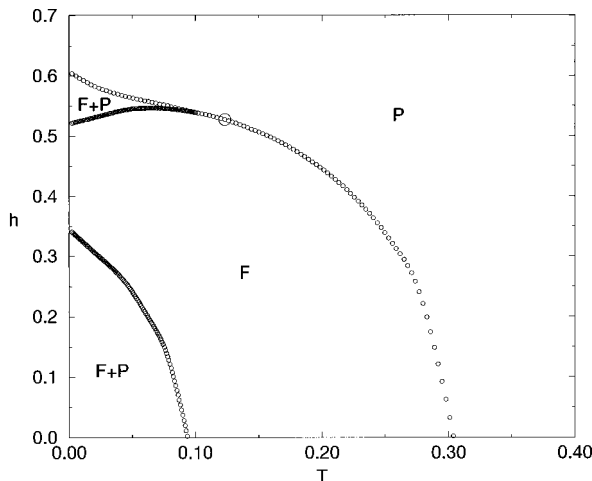
m_1 is very small, almost zero, such that both sublattices are practically uncoupled, leaving m_2 free to oscillate with the external field giving a paramagnetic-type response, $Q = 0$, as seen in Fig. 5. When $D \leqslant -2.037\,60$ the phase diagram changes dramatically. The paramagnetic region is extended over the low h regions, new critical lines appear, and a second dynamical tricritical point emerges. Phase diagrams in this interval can be observed in Fig. 6. The two first order transitions that occur at low temperature and the two second order transitions at higher temperature are shown in Fig. 7. In all cases we found that, as the crystalline field D becomes larger but negative, the region of the phase space where the system behaves ferromagnetically becomes narrower and shifts toward higher values of h. This effect, shown in the inset of Fig. 6, is somewhat expected since, for these values of D, higher values of h are needed to keep $m_1(\xi)$ different from zero such that the order parameter Q can also be different from zero. If D is large enough and negative, the system behaves in almost all the plane (T,h) as a paramagnet.

FIG. 4. Phase diagram in the plane (T,h) for $\Omega/2\pi = 1.0$ and $D = -1.5$. The $\bigcirc$ symbol indicates the dynamical tricritical point. Notice the appearance of a new critical line at low T.
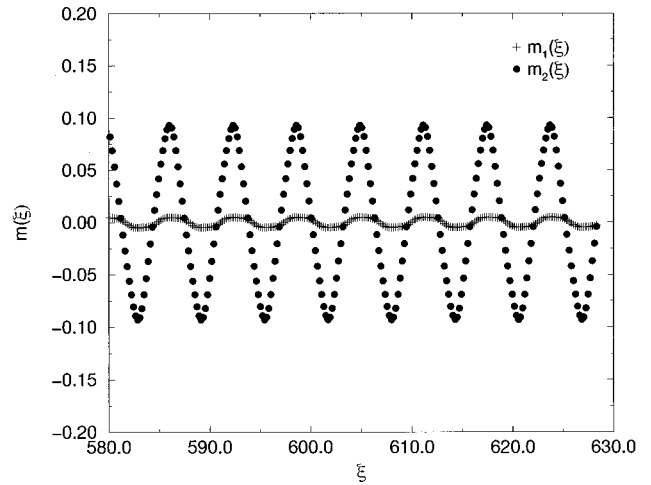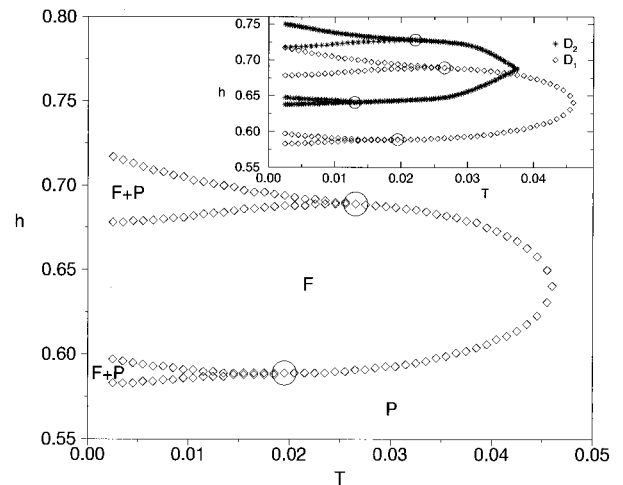

FIG. 6. Phase diagram in the plane (T,h) for $\Omega/2\pi = 1.0$ and $D = -2.5$. In the inset we compare the phase diagram for two values of D: $D_1 = -2.5$ and $D_2 = -2.7$. Again the $\bigcirc$ symbol indicates the dynamical tricritical points.

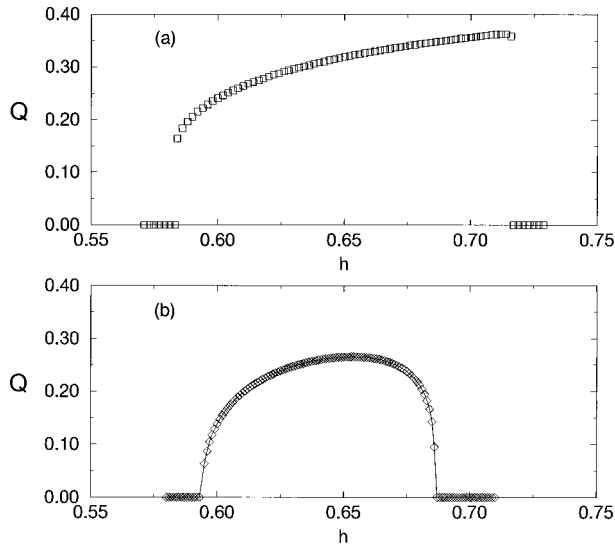FIG. 7. Order parameter Q as a function of the external magnetic field h for $\Omega/2\pi=1.0$ and $D=-2.5$; (a) for $T=0.0025$ and (b) for $T=0.0305$.

An interesting question arises at this point: is the existence of a second tricritical point due to the fact that our model has a higher spin value, $S=\pm 1,0$, than the Ising model, or to the fact that the S- and σ-spin operators are alternated on the lattice? To address this point, we study the Blume-Capel model (BC) where a spin $S=\pm 1,0$ is located at each site of a square lattice. The Hamiltonian of the BC model is

$$\mathcal{H}=-J\sum_{\langle NN\rangle} S_iS_j-D\sum_i S_i^2-H\sum_i S_i, \qquad (20)$$

where J, D, and H are in energy units. We choose $J=-1$ in order to compare with our model. Applying the Glauber-type stochastic dynamics and the mean-field approach described in Sec. II B, we get that the time evolution of the BC model is given by
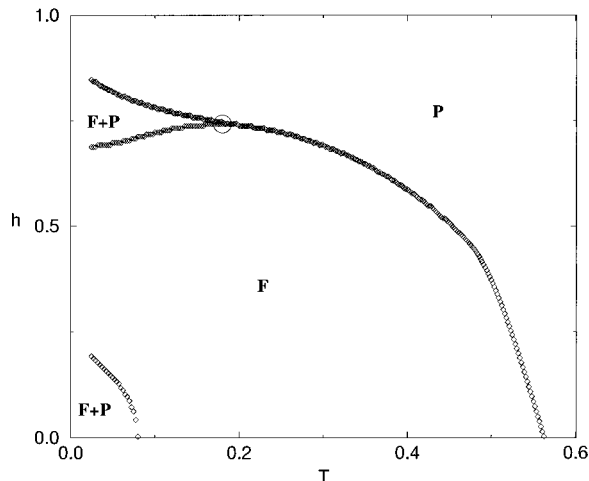

FIG. 8. Phase diagram of the Blume-Capel model in the plane (T,h) for $\Omega/2\pi=1.0$ and $D=-1.0$. Again the $\bigcirc$ symbol indicates the dynamical tricritical point.
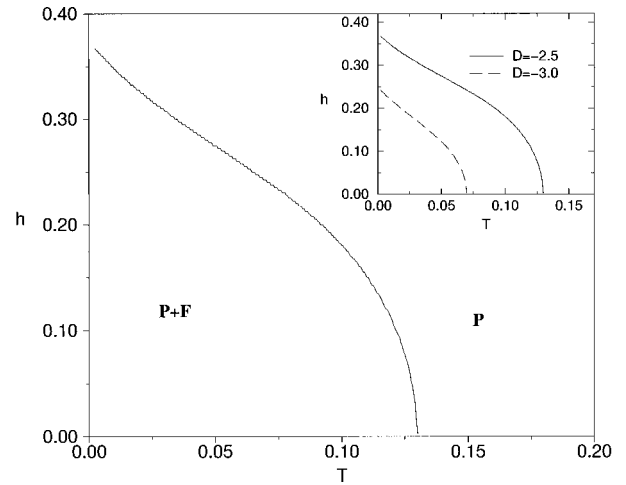

FIG. 9. Phase diagram of the Blume-Capel model in the plane (T,h) for $\Omega/2\pi=1.0$ and $D=-2.5$. In the inset we compare the phase diagram for two values of D: -2.5 and -3.0.

$$\Omega\frac{d}{d\xi}m=-m+\frac{\sinh(1/T)(m+h\cos\xi)}{\cosh(1/T)(m+h\cos\xi)+\frac{1}{2}\exp(-\beta D)}, \qquad (21)$$

where $m=\langle S_i\rangle$ is the total magnetization.

The numerical solution of Eq. (21) shows that, when $D\geq 0$ the BC model has an Ising-type behavior: it has only one dynamical tricritical point [12]. When D is very small and negative it behaves as our mixed Ising model: it exhibits a new first order critical line for low temperatures, as can be seen in Fig. 8. However, as D becomes larger but negative, the behavior of the BC model departs completely from the mixed model: the second order critical line disappears and, not only a new tricritical point does not appear, but the old one disappears, as can be seen in Fig. 9. This study indicates that the existence of a second tricritical point is not simply due to the fact that our model has a higher spin operator but to the mixing of the two types of spins.

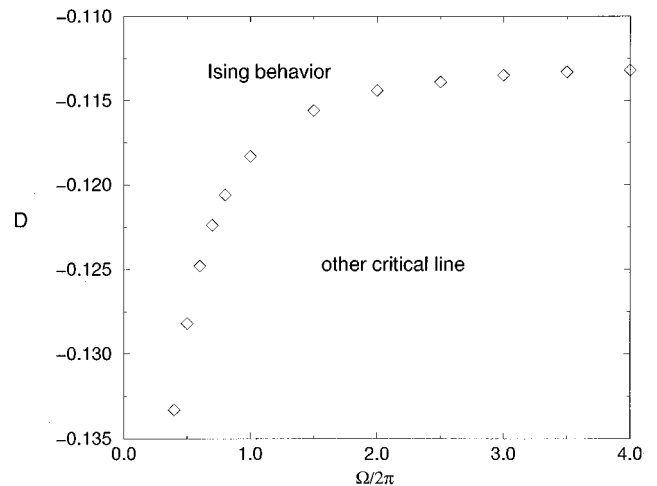All the results shown have been obtained with $\Omega/2\pi=1.0$, however, we repeated our studies for different values

FIG. 10. Dependence between the minimum value of D at which the system departs from the standard Ising model by the appearance of the other critical line, and the frequency $\Omega/2\pi$.

of $\Omega/2\pi$ and obtained qualitatively the same results. We found that the value of $D = -2.037\,60$, at which the system starts to exhibit two dynamical tricritical points, is independent of the frequency, but the value of D at which the model departs from the standard Ising model by the appearance of a second critical line depends on the frecuency as shown in Fig. 10. We found that, independently of the value of D, when $\Omega \rightarrow 0$ the region where both solutions coexist P+F vanishes and the tricritical temperature approaches the static critical value.

IV. CONCLUSIONS

We have analyzed within a mean-field approach the kinetics of a classical mixed Ising ferrimagnetic model in the presence of a time-dependent oscillating external field. We use a Glauber-type stochastic dynamics to describe the time evolution of the system. We found that the behavior of the system strongly depends on the values of the crystal field parameter, D. For large and positive values of D the system behaves as the standard Ising model [11], it has a continuous phase transition at high T and low h. As T decreases and h increases the transition becomes discontinuous and the system presents a dynamical tricritical point, see Fig. 3. However, when D is large enough and negative the phase diagram changes completely. First, a new critical line appears at

low T that marks a discontinuous phase transition between a new coexistence region P+F and the F region. As D becomes larger (and negative) the ferromagnetic region shrinks, the paramagnetic region also covers the low h region, new critical lines appear, and a second dynamical tricritical point emerges, see Fig. 6. The minimum value of $|D|$ at which the new tricritical point appears seems to be independent of Ω (for $\Omega \neq 0$).

A similar study on the Blume-Capel model ($S = \pm 1, 0$) reveals that the behavior of our mixed ferrimagnetic model, in particular the appearance of two tricritical points, is intimately related to the mixing of the two types of spin operators, and not only due to the fact of having a higher spin operator.

This mean-field study suggests that the mixed Ising ferrimagnetic model has an interesting dynamical behavior, quite different from the standard Ising model, and it would be worthwhile to further explore it with more accurate techniques such as Monte Carlo simulations or renormalization-group calculations.

ACKNOWLEDGMENTS

[1] R. J. Glauber, J. Math. Phys. **4**, 294 (1963).

[2] M. Acharyya and B. K. Chakrabarti, in *Annual Reviews of Computational Physics I*, edited by D. Stauffer (World Scientific, Singapore 1994); W. S. Lo and R. A. Pelcovits, Phys. Rev. A **42**, 7471 (1990); H. L. Richards, M. A. Novotny, and P. A. Rikvold, Phys. Rev. B **54**, 4113 (1996).

[3] S. W. Sides, R. A. Ramos, P. A. Rikvold, and M. A. Novotny, J. Appl. Phys. **79**, 6482 (1996); **81**, 5597 (1997).

[4] *Magnetic Molecular Materials*, Vol. 198 of NATO ASI Series E, edited by D. Gatteschi, O. Kahn, J. S. Miller, and F. Palacio (Kluwer Academic, Dordrecht, 1991).

[5] G. J. A. Hunter, R. C. L. Jenkins, and C. J. Tinsley, J. Phys. A **23**, 4547 (1990); R. G. Bowers and B. Y. Yousif, Phys. Lett. **96A**, 49 (1983).

[6] S. L. Schofield and R. G. Bowers, J. Phys. A **13**, 3697 (1980).

[7] T. Kaneyoshi, Solid State Commun. **70**, 975 (1989).

[8] G. M. Buendía and M. A. Novotny, J. Phys.: Condens. Matter **9**, 5951 (1997); G. M. Buendía and J. A. Liendo, *ibid.* **9**, 5439 (1997).

[9] K. Binder, in *Monte Carlo Methods in Statistical Physics*, edited by K. Binder (Springer, Berlin, 1979), Vol. 7, p. 1.

[10] M. Suzuki and R. Kubo, J. Phys. Soc. Jpn. **24**, 51 (1968).

[11] T. Tomé and M. J. de Oliveira, Phys. Rev. A **41**, 4251 (1990).

[12] F. Lee, B. Westwanski, Y. L. Wang, J. Appl. Phys. **53**, 1934 (1982); D. P. Landau and R. H. Swendsen, Phys. Rev. Lett. **46**, 1437 (1981).